Periodic Breathing in Heart Failure Explained by Dynamic and Static Properties of Respiratory Control

Tadayoshi Miyamoto[1], Hidehiro Nakahara[1], Shinya Ueda[1], Kou Manabe[1], Eriko Kawai[1], Masashi Inagaki[2], Toru Kawada[2] and Masaru Sugimachi[2]

[1]Graduate School of Health Sciences, Morinomiya University of Medical Sciences, Osaka City, Osaka, Japan. [2]Department of Cardiovascular Dynamics, National Cerebral and Cardiovascular Center, Suita City, Osaka, Japan.

Supplementary Issue: Heart Failure: An Exploration of Recent Advances in Research and Treatment

ABSTRACT

OBJECTIVE: The respiratory operating point is determined by the interplay between the controller and plant subsystem elements within the respiratory chemoreflex feedback system. This study aimed to establish the methodological basis for quantitative analysis of the open-loop dynamic properties of the human respiratory control system and to apply the results to explore detailed mechanisms of the regulation of respiration and the possible mechanism of periodic breathing in chronic heart failure.

METHODS AND RESULTS: In healthy volunteers, we measured arterial CO_2 partial pressure (Pa_{CO2}) and minute ventilation ($\dot{V}_E$) to estimate the dynamic properties of the controller ($Pa_{CO2} \rightarrow \dot{V}_E$ relation) and plant ($\dot{V}_E \rightarrow Pa_{CO2}$ relation). The dynamic properties of the controller and plant approximated first- and second-order exponential models, respectively, and were described using parameters including gain, time constant, and lag time. We then used the open-loop transfer functions to simulate the closed-loop respiratory response to an exogenous disturbance, while manipulating the parameter values to deviate from normal values but within physiological ranges. By increasing both the product of gains of the two subsystem elements (total loop gain) and the lag time, the condition of system oscillation (onset of periodic breathing) was satisfied.

CONCLUSION: When abnormality occurs in a part of the respiratory chemoreflex system, instability of the control system is amplified and may result in the manifestation of respiratory abnormalities such as periodic breathing.

KEYWORDS: systems analysis, respiratory abnormality, chemoreflex, negative feedback

Introduction

Ventilatory abnormalities are cardinal symptoms in patients with chronic heart failure (CHF). In CHF patients, enhanced ventilatory response to exercise,[1–3] Cheyne–Stokes respiration,[4–8] and periodic breathing[9–11] are associated with significantly higher mortality.

Ventilatory abnormalities appear to arise from pathophysiological changes in the respiratory chemoreflex system.[12,13]

In the presence of normal kidney function, ventilatory regulation maintains arterial CO_2 partial pressure (Pa_{CO2}) or pH at almost constant level, indicating that Pa_{CO2} serves as a controlled variable. The chemoreflex is a powerful feedback control system mediated by Pa_{CO2} and functions physiologically to maintain respiratory homeostasis. The system consists of two elements: controller and plant (Fig. 1). Theoretically, the unique values of minute ventilation ($\dot{V}_E$) and Pa_{CO2} are determined by the interaction between controller and plant system properties.[14–16] Recently, we have developed an experimental method (equilibrium diagram analysis) characterizing this feedback system by subdividing it into two subsystems in human volunteers.[17–20] Using this equilibrium diagram, we can analyze how the unique value of $\dot{V}_E$ is determined by the respiratory chemoreflex system, how changes in controller properties affect $\dot{V}_E$, or how changes in the plant properties affect $\dot{V}_E$.

However, the above framework has a limitation in evaluating the dynamic behavior of respiratory control against perturbations that vary constantly. There is a need to develop new methods to accurately identify the dynamic control function, which is essential to evaluate the integrated function of the respiratory feedback control system. Systematic evaluation of the integrated function would also help elucidate the mechanism of respiratory abnormalities in CHF patients with Cheyne–Stokes respiration and/or periodic breathing, in
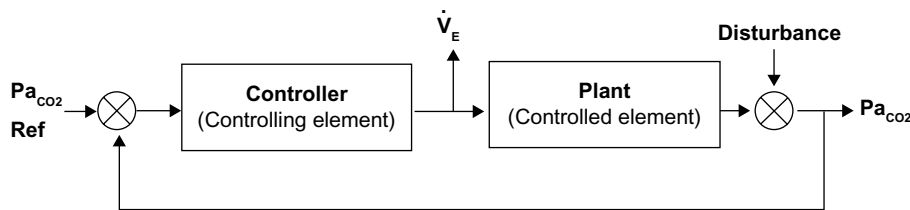
Figure 1. Respiratory chemoreflex feedback control system regulating carbon dioxide partial pressure. The respiratory chemoreflex system consists of two subsystems: the controller and the plant. In the controller, the input variable is arterial CO_2 partial pressure (Pa_{CO_2}) and the output variable is minute ventilation ($\dot{V}_E$). The controller can be characterized by observing changes in $\dot{V}_E$ in response to changes in Pa_{CO_2}. In the plant, the input variable is $\dot{V}_E$, and the output variable is Pa_{CO_2}. The plant can be characterized by observing changes in Pa_{CO_2} in response to changes in $\dot{V}_E$.

which instability of the negative feedback system is thought to be the main cause.[21]

Objective

With the above background, the present study aimed to establish a new methodology to quantify the dynamic control function of the human respiratory chemoreflex system and to discuss the pathophysiological relevance of the findings with respect to respiratory abnormalities in CHF.

Material and Methods

Subjects. Nine nonsmoking, nonobese healthy male subjects were studied. They were 20.4 ± 1.7 years (mean $\pm$ SD) in age, 173.1 ± 8.4 cm in height, and 63.8 ± 9.4 kg in weight. All the subjects provided written informed consent prior to participation in the study. The study was approved by the Human Subjects Committee of Morinomiya University of Medical Sciences (No. 001), which conforms to the Declaration of Helsinki. All the subjects had no known cardiovascular or pulmonary disorders and no head injuries, and were not using any prescribed medication known to influence systemic or cerebrovascular function.

Experimental procedures. Twenty-four hours prior to each experiment, the subjects were instructed to avoid strenuous exercise and to maintain their ordinary diet but to avoid food with a high salt content. Subjects arrived at the laboratory at least two hours after a light meal. Before starting the experiment, the subjects rested in a comfortable chair in the sitting position. A catheter (0.47 mm ID, 24 gage) was placed in the brachial artery of the nondominant arm for arterial blood sampling, and for arterial blood pressure measurement by connecting to a pressure transducer (DX-200, Nihon Kohden) positioned at the level of the right atrium in the midaxillary line, fastened to the subject, and connected to a pressure monitoring system (RM-6000, Nihon Kohden). The experiment started 20–30 minutes after the catheter was placed.

In order to characterize both the controller and plant properties, the participants sequentially underwent two experimental procedures in the sitting position: a resting hypercapnia test and a hyper/hypoventilation test, on the same day.

Measurement methods. (i) Quantitative analysis of static and dynamic properties of controller.

In the first experiment, a hypercapnia test was performed to quantify the dynamic properties of the controller by measuring breath-by-breath $\dot{V}_E$. This test consisted of three separate trials (fractional concentrations of inspired CO_2 [F_{ICO_2}] = 0.00, 0.035, and 0.05 and containing 40% O_2 balanced with N_2) as shown in Figure 2. Pretrial baseline data were recorded for a 5-minute period with the participant wearing a face mask attached to a Douglas bag containing 0% CO_2 and 40% O_2 balanced with N_2 at the prevailing barometric pressure. For the 0% F_{ICO_2} trial, the inspired gas was not changed for a total of 17 minutes. For the 3.5% and 5% F_{ICO_2} trials, 0% CO_2 was inspired for the initial five minutes, and then, CO_2 was increased in a one-step manner to 3.5% and 5% CO_2, respectively, and maintained for 12 minutes, during which $\dot{V}_E$ and end-tidal partial pressure of CO_2 (P_{ETCO_2}) were measured continuously using an expired gas analyzer (see Experimental measurements section). Each F_{ICO_2} trial lasted 12 minutes, with an inter-trial room air recovery period of 20 minutes. This duration is sufficient to permit CO_2 at the central chemoreceptors to reach a new steady state.[22–24] The order of the F_{ICO_2} trials was randomized for each subject.

Experimental protocol
Test procedures
1) Hypercapnia test (3 trials)
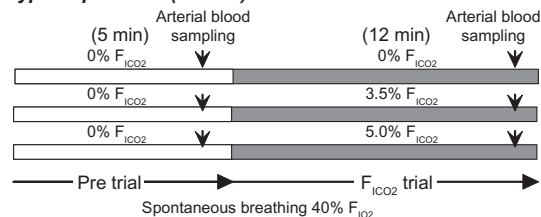
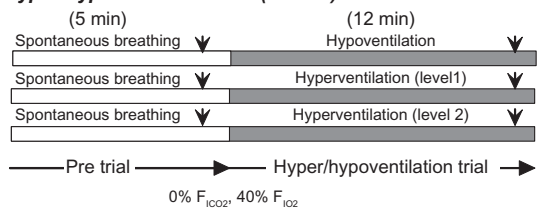*2) Hyper/hypoventilation test (3 trials)*

Figure 2. Experimental protocol. In both the hypercapnia test and the hyper/hypoventilation test, three trials were performed in random order.

A previous study indicates that a negative interaction exists between central and peripheral chemoreceptors for a single step of carotid body hypoxia.[25] In this study, all the trials were repeated under hyperoxic conditions in order to suppress the interaction from the O_2-sensitive chemoreflex.[25,26,31] Arterial blood was collected one minute before and 11 minutes after the CO_2 inspiration was started, and the Pa_{CO2} measured from each subject was used to calibrate the continuous P_{ETCO2} data and to obtain estimated Pa_{CO2} ($_{est}Pa_{CO2}$).

(ii) Quantitative analysis of static and dynamic properties of plant

In the second experiment, a hyper/hypoventilation test was performed to quantify the dynamic property of the plant by measuring breath-by-breath P_{ETCO2} responses to hyper/hypoventilation. Each hyper/hypoventilation test consisted of three trials (two levels of hyperventilation and one hypoventilation) as shown in Figure 2. After maintaining spontaneous breathing in the resting state for five minutes (inspired gas containing 0% CO_2 and 40% O_2 with N_2 balance), hyperventilation was induced voluntarily to change $\dot{V}_E$ in a one-step manner and maintained for 12 minutes. The subject was instructed to breathe voluntarily at different respiratory rate (RR) and tidal volumes to match a visual display of ventilation curves on a screen monitor.[17–20] For the two levels of hyperventilation, the subject breathed according to ventilation curves at RR and tidal volume (V_T) mimicking those recorded during the hypercapnia test trials. For one level of hypoventilation, the subject breathed following a breathing curve at 93% RR and 90% tidal volume when F_{ICO2} was 0.0. Each trial lasted 12 minutes, with interposing intervals of at least 20 minutes during which the subject breathed room air. All the trials were started after $\dot{V}_E$ and P_{ETCO2} had recovered to baseline levels. All the trials were repeated under hyperoxic condition ($F_{ICO2} = 0.0$, $F_{IO2} = 0.40$ with N_2 balance). The order of the trials was randomized for each subject. Arterial blood was collected one minute before and 11 minutes after hypo/hyperventilation was started, and the Pa_{CO2} measured from each subject was used to calibrate the continuous P_{ETCO2} data and to obtain $_{est}Pa_{CO2}$.

Experimental measurements. Signals from a respiratory gas analyzer (ARCO2000-MET, Arcosystem) and an electrocardiograph (BSM-7201, Nihon Kohden) were synchronized online using a personal computer and continuously displayed during the experiment. Oxygen and CO_2 measurements were calibrated using a standard gas of known concentrations before each test. Heart rate (HR) and mean blood pressure (MBP) were monitored using a lead II electrocardiogram and a pressure monitoring system (RM-6000, Nihon Kohden). Ventilatory responses were measured using a non-rebreathing open circuit apparatus (Model 8250, Hans Rudolph). The subject breathed through a face mask attached to a low-resistance one-way valve with a flow meter (ARCO2000-MET, Arcosystem). The valve mechanism allowed the subject to inspire room air or a selected gas mixture from a 200-L Douglas

bag containing 0.0%, 3.5%, or 5.0% CO_2 in 40% O_2 with N_2 balance. The total apparatus dead space was 200 mL. Respiratory and metabolic data during the experiments were recorded using an automatic breath-by-breath respiratory gas analyzing system. We digitized expired flow, CO_2 and O_2 concentrations, and derived V_T, RR, $\dot{V}_E$, and P_{ETCO2}. Flow signals were computed to single breath data and matched to gas concentrations identified as single breaths using P_{ETCO2}, after correcting the time lag (350 ms) arising from the length of sampling tube in gas concentration measurements. The corresponding O_2 uptake (V_{O2}) and CO_2 output (V_{CO2}) for each breath were calculated from inspired–expired gas concentration differences, and by expired ventilation, with inspired ventilation being calculated by N_2 correction. During each protocol, HR, MBP, $\dot{V}_E$, P_{ETO2}, and P_{ETCO2} were recorded continuously at 200 Hz. Arterial CO_2 and O_2 partial pressures and pH were measured anaerobically using a blood gas analyzer (IL 1620, Instrumentation Laboratory Co.).

Data analysis. Steady-state $\dot{V}_E$ and P_{ETCO2} data were obtained by averaging the respective data for the last two minutes. To quantify the static property of the controller ($Pa_{CO2} \rightarrow \dot{V}_E$ relation), we performed linear regression of $\underline{V}_E$ against Pa_{CO2} as follows

$$\dot{V}_E = S \cdot (Pa_{CO2} - B) \qquad (1)$$

where S is the slope and B is the Pa_{CO2}-intercept.[27] To characterize the dynamic property of the controller, the step response of $\dot{V}_E$ to a change in F_{ICO2} was modeled by the following equation:

$$\dot{V}_E(t) = \dot{V}_E(0) + G_u \cdot \left[1 - exp\left(-\frac{t - L_u}{\tau_u}\right)\right] \cdot \Delta_{est}Pa_{CO2} \qquad (2)$$

where G_u, τ_u, and L_u represent the steady-state gain, time constant, and lag time, respectively. $\Delta_{est}Pa_{CO2}$ represents the difference between the steady-state $_{est}Pa_{CO2}$ and the baseline $_{est}Pa_{CO2}$. $\dot{V}_E(0)$ represents the baseline $\dot{V}_E$, which may be determined from the baseline Pa_{CO2} based on Equation 1. Assuming that $_{est}Pa_{CO2}$ is equal to Pa_{CO2}, G_u is nothing but another representation of the controller gain, S, in Equation 1. In this estimation of the dynamic property of the controller, a delay in the $_{est}Pa_{CO2}$ response to a step change in F_{ICO2} was ignored because the time constant for the $_{est}Pa_{CO2}$ step response (approximately 20 seconds) was much shorter than that for the $\dot{V}_E$ step response (approximately 120 seconds, see Results section, Fig. 4).

To quantify the static property of the plant ($\dot{V}_E \rightarrow Pa_{CO2}$ relation), we fitted the following equation to the measured data, including normal spontaneous breathing data

$$Pa_{CO2} = \frac{A}{\dot{V}_E} + C \qquad (3)$$

which is modified from the original metabolic hyperbola[17] and is referred to as the modified metabolic hyperbola hereafter in the present paper. A and C are constants for the numerator of the hyperbola and the asymptote, respectively. To characterize the dynamic property of the plant, the step response of $_{est}Pa_{CO_2}$ to a change in the visual display command of the ventilation curve was modeled by the following equation

$$_{est}Pa_{CO_2}(t) = {}_{est}Pa_{CO_2}(0) + \left\{ G_{v1} \cdot \left[1 - exp\left(-\frac{t - L_{v1}}{\tau_{v1}} \right) \right] \right.$$
$$\left. + G_{v2} \cdot \left[1 - exp\left(-\frac{t - L_{v2}}{\tau_{v2}} \right) \right] \right\} \cdot \Delta\dot{V}_E \quad (4)$$

where G_{v1}, τ_{v1}, and L_{v1} represent the steady-state gain, time constant, and lag time, respectively, for the first exponential; G_{v2}, (τ_{v2}, and L_{v2} represent the steady-state gain, time constant, and lag time, respectively, for the second exponential. (ΔV_E represents the difference between the steady-state ΔV_E and the baseline ΔV_E. $_{est}Pa_{CO_2}(0)$ represents the baseline $_{est}Pa_{CO_2}$. Considering the breath-by-breath nature of the raw ΔV_E values, a deviation of the ΔV_E change from an ideal step input was ignored in the estimation of the dynamic property of the plant. Actually, ΔV_E was changed almost instantly according to the step change in the visual display command of the ventilation curve in the subjects under study who had been familiarized with the method.

The measured operating point for each subject was defined as the steady-state values of $\dot{V}_E$ and Pa_{CO_2} obtained in the trial of $F_{ICO_2} = 0.00$ without visual feedback (ie, during spontaneous breathing). The plant gain (G_p) was calculated as the tangential slope of the modified metabolic hyperbola at the operating point. Mathematically speaking, the sum of G_{v1} and G_{v2} determined from a small $\Delta\dot{V}_E$ should correspond

to G_p at the baseline $\dot{V}_E$. The total loop gain (TG) at the operating point was estimated by the product of the gains of the controller and the plant.

Statistical analysis. Parameters for the controller and plant elements were analyzed by fitting respective models to the response curves via linear and nonlinear least-squares regression analyses. Pearson product-moment correlations were calculated between P_{ETCO_2} values and the corresponding Pa_{CO_2} data. All the data are presented as mean ± SD.

Results

Table 1 summarizes the cardiorespiratory and blood gas responses during the 0% F_{ICO_2} and 5% F_{ICO_2} trials in the hypercapnia test and the hyperventilation trial in the hyper/hypoventilation test. Both hypercapnia and hyperventilation increased $\dot{V}_E$, V_T, RR, HR, and Pa_{O_2} ($P < 0.01$). MBP was increased only by hyperventilation ($P < 0.01$). The 5% F_{ICO_2} trial increased P_{ETCO_2} and Pa_{CO_2} ($P < 0.01$), whereas the hyperventilation trial decreased P_{ETCO_2} and Pa_{CO_2} ($P < 0.01$).

Quantitative analysis of static properties of controller and plant. The left panels of Figure 3, which are diagrams of static properties of the controller (Fig. 3A) and plant (Fig. 3C) and the equilibrium diagram (Fig. 3E) derived from a representative subject are shown. The right panels show pooled data from all the subjects. As shown in Figure 3A and B, $\dot{V}_E$ increased linearly with Pa_{CO_2} increase both in the representative case and in pooled data. The slope of the regression line for pooled data, which represents the controller gain, was 2.0 ± 1.3 L minute^{-1} mmHg^{-1}, and the Pa_{CO_2}-intercept was 31.9 ± 20.3 mmHg. The effect of changes in $\dot{V}_E$ on Pa_{CO_2} is shown in Figure 3C and D. The relationship approximated a modified metabolic hyperbola reasonably well. The mean value of the numerator of the hyperbola was 329 ± 129 L minute^{-1} mmHg with an asymptote of 14.2 ± 7.1 mmHg. The plant gain at the measured operating point was -2.6 ± 1.2 mmHg L^{-1} minute.

Table 1. Steady-state cardiorespiratory and blood gas responses during 0% F_{ICO2}, 5% F_{ICO2}, and hyperventilation trials.

		SPONTANEOUS BREATHING		HYPERCAPNIA TEST		HYPER/HYPOVENTILATION TEST	
		PRE-TRIAL	0% F_{ICO2} TRIAL	PRE-TRIAL	5% F_{ICO2} TRIAL	PRE-TRIAL	HYPERVENTILATION TEST
$\dot{V}_E$	(L/min)	11.0 ± 1.5	11.5 ± 1.6	10.9 ± 2.1	25.2 ± 6.9**	11.4 ± 2.3	25.1 ± 6.6**
P_{ETCO2}	(mmHg)	39.1 ± 2.5	39.0 ± 3.3	39.0 ± 2.7	50.4 ± 2.4**	39.0 ± 4.1	23.0 ± 4.5**
V_T	(mL)	1018 ± 727	1024 ± 759	864 ± 316	1446 ± 332**	931 ± 384	1390 ± 411**
RR	(breaths/min)	13.2 ± 3.7	14.2 ± 4.7	14.4 ± 4.5	18.5 ± 5.5**	14.4 ± 5.2	19.2 ± 5.4**
HR	(beats/min)	63.7 ± 14.3	65.2 ± 12.1	63.7 ± 15.4	68.2 ± 14.5**	69.7 ± 12.1	78.7 ± 12.5**
MBP	(mmHg)	89.9 ± 16.1	92.8 ± 14.0	88.2 ± 16.2	92.2 ± 14.9	90.3 ± 15.1	98.7 ± 12.4**
pH		7.39 ± 0.02	7.39 ± 0.03	7.39 ± 0.02	7.35 ± 0.02**	7.41 ± 0.02	7.58 ± 0.05**
Pa_{O2}	(mmHg)	241 ± 7	239 ± 12	239 ± 7	278 ± 7**	240 ± 6	264 ± 6**
Pa_{CO2}	(mmHg)	43.8 ± 3.9	44.0 ± 3.9	44.5 ± 3.9	51.2 ± 3.1**	43.6 ± 2.6	26.0 ± 42**

Notes: Values are means ± SD **$P < 0.01$ vs Pre-trial.
Abbreviations: $\dot{V}_E$, minute ventilation; P_{ETCO2}, end-tidal partial pressure of carbon dioxide; V_T, tidal volume; RR, respiratory rate; HR, heart rate; MBP, mean blood pressure; Pa_{O2}, partial pressure of oxygen in arterial blood; Pa_{CO2}, partial pressure of carbon dioxide in arterial blood.
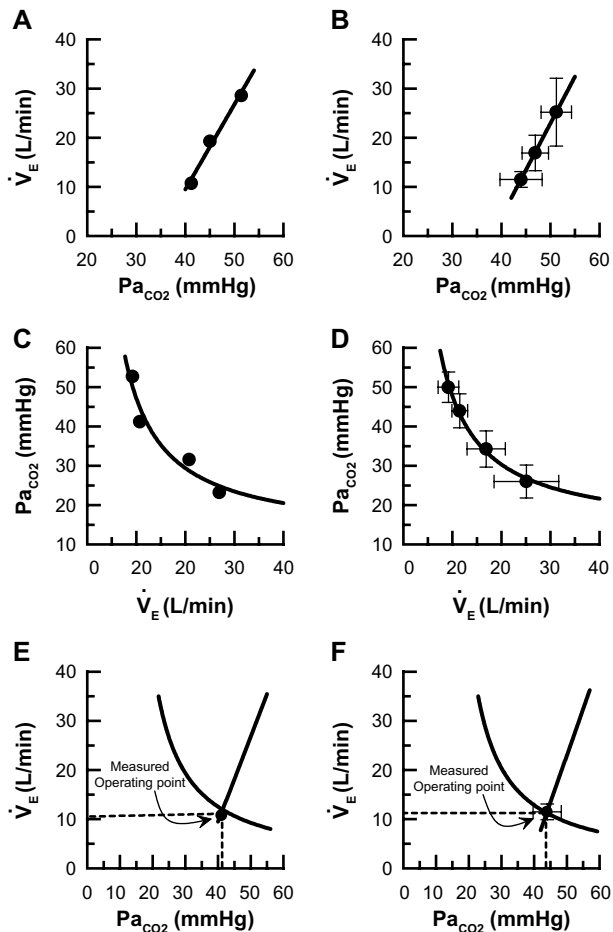
Figure 3. Static properties of the controller and the plant, and the equilibrium diagram derived from a representative case (left panels) and pooled data from all subjects (right panels). In the pooled data, horizontal and vertical bars indicate mean ± SD. Panels **A** and **B**: minute ventilation ($\dot{V}_E$) increased linearly with increase in arterial CO_2 partial pressure (Pa_{CO2}). The averaged regression line for the pooled data was $\dot{V}_E = 2.0 \times (Pa_{CO2} - 31.9)$. Panels **C** and **D**: The plant was characterized by a modified metabolic hyperbola. The best-fit hyperbola for the pooled data was $Pa_{CO2} = 329/\dot{V}_E + 14.2$. Panels **E** and **F**: The operating points estimated from the equilibrium diagram were very close to those measured, both in the representative case and in pooled data.

Since we can characterize both the controller and plant with the common variables of $\dot{V}_E$ and Pa_{CO2}, the operating point can be estimated as the intersection between the two operational lines on the equilibrium diagrams (Fig. 3E and F). The respiratory TG at the operating point was 5.6 ± 3.6.

Quantitative analysis of dynamic properties of controller and plant. In the first experiment, we measured $_{est}Pa_{CO2}$, V_T, and RR in response to a one-step increase in F_{ICO2}. $\dot{V}_E$ was calculated from the product of V_T and RR, and $_{est}Pa_{CO2}$ was estimated by continuous P_{ETCO2} and Pa_{CO2} relations. By inspiring the CO_2-containing gas, $_{est}Pa_{CO2}$ also showed a corresponding one-step increase and was accompanied by increases in V_T and RR in both the representative case (Fig. 4A) and pooled data (Fig. 4B). As a result, $\dot{V}_E$ increased in an exponential manner. The $\dot{V}_E$ step response can be approximated by a first-order

low-pass filter ($r^2 = 0.749 \pm 0.17$, ranging from 0.479 to 0.926) (Fig. 5A). The coefficients were estimated as follows: $\dot{V}_E(0)$; 10.9 ± 2.1 L minute^{-1}, gain G_u; 2.9 ± 1.8 L minute^{-1} mmHg^{-1}, lag time L_u; 3.3 ± 4.9 seconds, time constant τ_u; 119 ± 48 seconds, $\Delta_{est}Pa_{CO2}$; 6.7 ± 2.6 mmHg.

In the second experiment, we measured $_{est}Pa_{CO2}$ in response to a one-step increase in $\dot{V}_E$ by voluntarily changing the RR and tidal volume. The $_{est}Pa_{CO2}$ step response can be approximated by a second-order low-pass filter in both the representative case (Fig. 4C) and pooled data (Fig. 4D), showing a biphasic response with a rapid decline in the initial phase of step loading followed by a gradual decrease ($r^2 = 0.899 \pm 0.07$, ranging from 0.742 to 0.966) (Fig. 5B). The coefficients were estimated as follows: $_{est}Pa_{CO2}(0)$; 44.3 ± 1.9 mmHg, gain G_{v1}; −0.6 ± 0.3 mmHg L^{-1} minute, gain G_{v2}; −1.1 ± 0.6 mmHg L^{-1} minute, lag time L_{v1}; 0.8 ± 1.1 seconds; lag time L_{v2}; 0.5 ± 0.6 seconds; time constant τ_{v1}; 11.9 ± 10.9 seconds, time constant τ_{v2}; 214 ± 101 seconds, $\Delta\dot{V}_E$; 13.5 ± 6.0 L^{-1} minute.

Simulation analysis of the closed-loop dynamic properties of the respiratory chemoreflex negative feedback system. Once open-loop static and dynamic characteristics of the controller and plant are identified, we can simulate the behavior of the respiratory chemoreflex control system under closed-loop conditions. Figure 6 shows the time course of Pa_{CO2} response to a one-step perturbation (step load: $Pa_{CO2} = 5$ mmHg) when the biological negative feedback loop is closed. Simulations were repeated while changing the dynamic property of the controller by setting different values for the gain and time constant. Because the controller and the plant are serially connected (Fig. 1), changes in the controller gain are proportional to changes in the TG of the system. The respiratory chemoreflex control system minimizes the effect of the perturbation by amplifying the difference between the present value and the negative feedback signal (error signal), and then feeding back. In the case that the system gain is attenuated from normal, or the time constant is prolonged from normal, or both, recovery of Pa_{CO2} after the perturbation (step load of Pa_{CO2}) takes a longer time. Conversely, in the case that the system gain is increased and time constant is shortened, the Pa_{CO2} recovery time becomes shorter but Pa_{CO2} shows marked fluctuation before it reaches a steady state, indicating decreased stability of the system.

Figure 7 illustrates the simulation results showing the time course of $\dot{V}_E$ in response to a one-step perturbation (step load: $Pa_{CO2} = 5$ mmHg). Simulations were repeated while changing the dynamic property of the controller by varying the gain and lag time. Because the controller and the plant are serially connected (Fig. 1), changes in the controller gain are proportional to changes in the TG of the system. Increases in TG and lag time from their normal values result in instability of the system, and abnormal findings such as periodic breathing (asterisks in Fig. 7) found in CHF can be observed in these simulations.
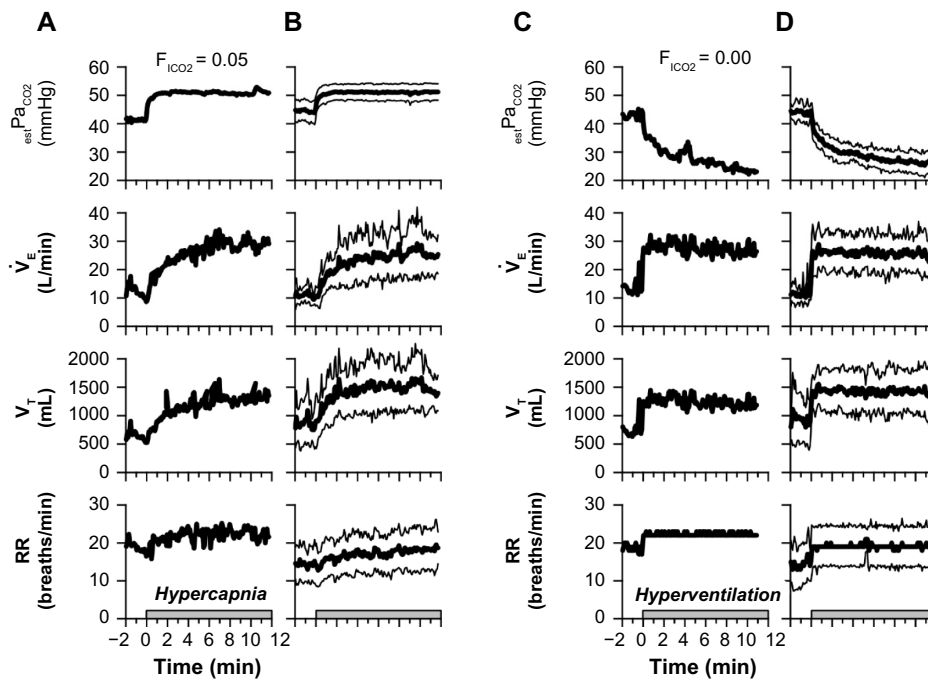
Figure 4. Time course of respiratory responses to a one-step increase in fractional concentration of inspired CO_2 (F_{ICO2}) or minute ventilation ($\dot{V}_E$) derived from a representative case (panels **A** and **C**) and pooled data from all subjects (panels **B** and **D**). For panels **A** and **B**, arterial blood was collected one minute before and 11 minutes after CO_2 inhalation (5% CO_2 in 40% O_2 with N_2 balance). For panels **C** and **D**, arterial blood was collected one minute before and 11 minutes after the change in ventilation pattern. The arterial CO_2 partial pressure (Pa_{CO2}) measured from each individual was used to calibrate the continuous end-tidal CO_2 partial pressure (P_{ETCO2}) data and to obtain estimated Pa_{CO2} ($_{est}Pa_{CO2}$).
Abbreviations: $\dot{V}_E$, minute ventilation, V_T, tidal volume; RR, respiratory rate.

Discussion

The dynamic properties of a regulatory system can be represented by transfer functions plotting gain and phase in the frequency domain. The time-domain counterpart of the transfer function is an impulse response. The step response is derived from a time integral of the impulse response. Therefore, the transfer function and step response are theoretically equivalent in describing the properties of a regulatory system. In the present study, we constructed a dynamic characteristic model using step response, based on the methodology developed in our previous study.[17–20] The following factors are implicated as causes of respiratory abnormality in CHF: (1) the central and peripheral chemoreflex sensitivity (controller gain) is often greatly increased and (2) the slowed circulation increases the delay in transmission of blood from the lungs to the brain, thus reducing the effectiveness of the damping system. Therefore, based on the quantitative analysis and simulation of the dynamic function of the respiratory chemoreflex system, we attempted to explain the mechanism of respiratory abnormalities in CHF. A previous study indicates that a negative interaction exists between central and peripheral chemoreceptors for a single step of carotid body hypoxia[25] and suggests that the negative interaction may contribute to respiratory abnormalities. However, we constructed a simple model of respiratory control, excluding the interaction from the peripheral chemoreceptors, in order to simplify the interpretation for our experimental model.

Quantitative analysis of dynamic and static properties of the respiratory chemoreflex negative feedback system. The present quantitative analysis approximated the controller element ($Pa_{CO2} \rightarrow \dot{V}_E$ relation) by a first-order exponential model with lag time and the plant element ($\dot{V}_E \rightarrow Pa_{CO2}$ relation) by a second-order exponential model with lag time, thereby describing the dynamic property of each element quantitatively using a set of parameters consisting of gain, time constant, and lag time.

The parameters of the aforementioned model equations are known to be determinants of rapidity and stability for the total negative feedback system.[14,28] For example, the input/output ratio, ie, gain, can be used to evaluate quantitatively the stability of a system. A larger gain implies high sensitivity to CO_2 in the controller and/or high CO_2 excretion capacity in response to ventilation in the plant. In our present data, the steady-state gains obtained for the controller and the plant at the operating point were 2.0 ± 1.3 L minute^{-1} mmHg^{-1} and -2.6 ± 1.2 mmHg L^{-1} minute, respectively.

In the field of system engineering, TG at the operating point is considered to be an "indicator of stability of the control system" and is represented by the product of the gains (slopes) at the operating points of all the subsystem elements. The TG of the respiratory chemoreflex feedback system calculated from the data of the present study is 5.6 ± 3.6. This TG value was consistent with our previous observation in human beings.[17] According to the feedback control theory described
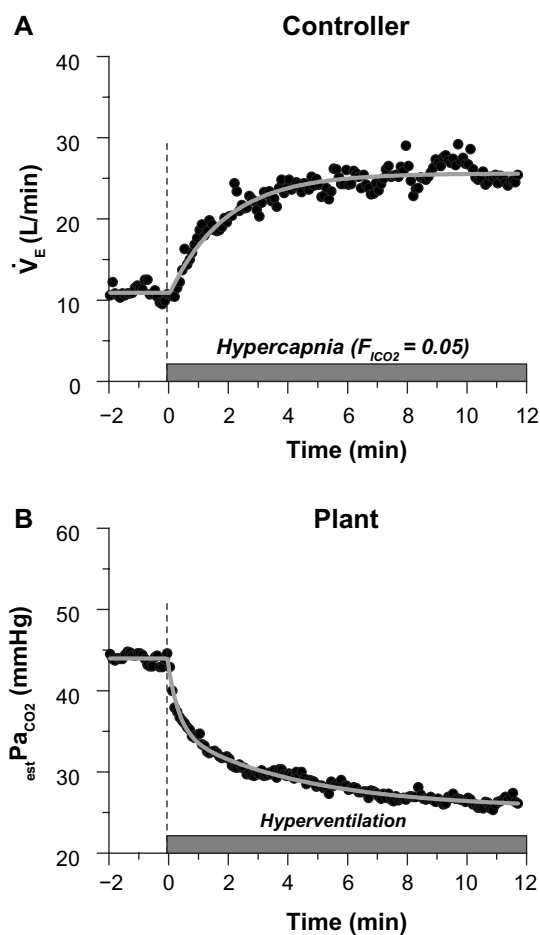
A Controller

B Plant

Figure 5. Typical dynamic properties (transient response properties) of the controller (**A**) and the plant (**B**) in the respiratory chemoreflex system. Arterial blood was collected one minute before and 11 minutes after the one-step intervention, and the arterial CO_2 partial pressure (Pa_{CO2}) measured from each individual was used to calibrate the continuous end-tidal CO_2 partial pressure (P_{ETCO2}) data and to obtain estimated Pa_{CO2} ($_{est}Pa_{CO2}$). In panel **A**, the controller property ($_{est}Pa_{CO2} \rightarrow \dot{V}_E$ relation) can be approximated by a first-order low-pass filter (the gray smooth line). The coefficients were estimated as follows: $\dot{V}_E(0)$; 10.9 ± 2.1 L minute^{-1}, gain G_u; 2.9 ± 1.8 L minute^{-1} mmHg^{-1}, lag time L_u; 3.3 ± 4.9 seconds, time constant τ_u; 119 ± 48 seconds, $\Delta_{est}Pa_{CO2}$; 6.7 ± 2.6 mmHg. In panel **B**, the plant element ($\dot{V}_E \rightarrow _{est}Pa_{CO2}$ relation) can be approximated by a second-order low-pass filter (the gray smooth line), showing a biphasic response with a rapid decline in the initial phase of step loading followed by a gradual decrease. The coefficients were estimated as follows: $_{est}Pa_{CO2}(0)$; 44.3 ± 1.9 mmHg, gain G_{v1}; -0.6 ± 0.3 mmHg L^{-1} minute, gain G_{v2}; -1.1 ± 0.6 mmHg L^{-1} minute, lag time L_{v1}; 0.8 ± 1.1 seconds; lag time L_{v2}; 0.5 ± 0.6 seconds; time constant τ_{v1}; 11.9 ± 10.9 seconds, time constant τ_{v2}; 214 ± 101 seconds.

variation in a process control,[14] proving that the biological respiratory system is an excellent system that is appropriately controlled even from the system engineering point of view.

The results of the simulation analyses shown in Figure 6 reveal that the dynamic nature of the negative feed-back open-loop properties is a factor determining the rapidity and stability of the response of the total negative feedback system. The respiratory chemoreflex system possesses a mechanism of Pa_{CO2} stabilization with adequate rapidity and stability when the system is examined using normal parameter values at the operating point.

Exploration of the mechanism of Cheyne–Stokes respiration or periodic breathing in heart failure patients. Although TG at the phase delay of π radians is considered to be an indicator of stability of the respiratory control system,[28] the value of TG higher than unity could induce respiratory abnormalities if excessive circulatory delay exists. Cheyne–Stokes respiration[4–8] and periodic breathing[9–11] are some examples of instability observed in biological respiratory control. The symptoms of these phenomena are repeated hyperventilation and apnea (or hypopnea) occurring in cycles of several seconds to tens of seconds.

The mechanisms of their occurrence have been attributed to a change in sensitivity to carbon dioxide (gain) or an increase in lung–chemoreceptor circulation time associated with central respiratory disorder. Especially, in CHF patients, the increase in central and peripheral chemoreflex sensitivity (controller gain) and the increase in peripheral plant gain because of an increase in dead space/tidal volume ratio are speculated to cause a TG increase in the system.[12,13,29] Additional factors that further exacerbate the stability of the whole system include the increase in lung–chemoreceptor blood transit time (increase in lag time) associated with decreases in cardiac output and ejection fraction,[7] and the increase in time delay that reflects Pa_{CO2} in brain tissue because of lowered cerebral blood flow.[30] Another factor is reduction of the functional residual capacity as a result of pulmonary edema in CHF. All these factors may predispose respiratory abnormalities such as periodic breathing.[14]

In this study, we performed simulation by fitting coefficients based on the data of dynamic properties obtained from healthy adults. When TG becomes excessively large, the ventilatory response to a change in Pa_{CO2} is accelerated, whereas an increase in gain alone leads to instability of the system causing an oscillatory phenomenon (Fig. 6). Furthermore as mentioned earlier, when the additional condition of prolonged lung–chemoreceptor blood transit time because of heart failure (increase in lag time) is fulfilled, the instability of the system is expected to be further amplified. In the simulation, when the system gain (up to three-fold increase) and lag time (prolongation up to 20 seconds) are both increased within a physiologically relevant range, the condition for system oscillation is satisfied and periodic breathing occurs (oscillation phenomenon) (Fig. 7).
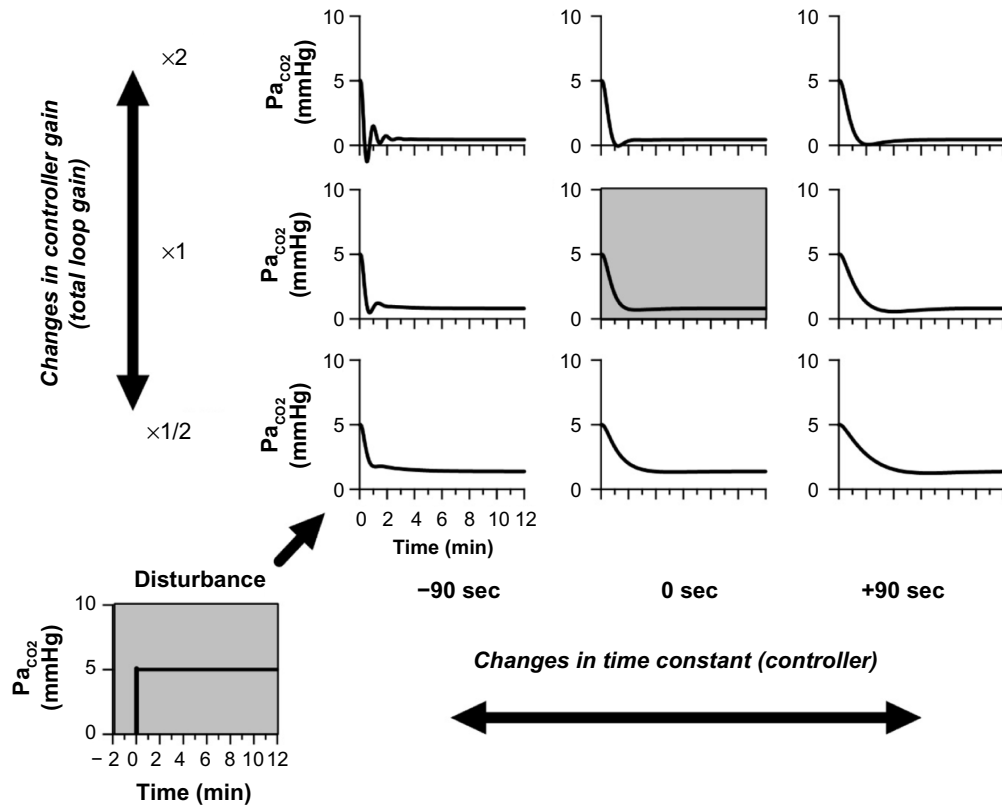
in a textbook written by Milhorn,[14] the perturbation imposed on the system is compressed to 1/(TG + 1) if the system is stable. In the respiratory system, TG = 5.6 implies that when a Pa_{CO2} perturbation with an amplitude of 10 mmHg is imposed on the system, the final observed change in Pa_{CO2} level (steady-state response) would be 1.5 mmHg. This TG value not only shows that the system is adequately stable but also that it approaches the value estimated for disturbance

Figure 6. Simulations of changes in arterial CO_2 partial pressure (Pa_{CO2}) over time when a one-step perturbation (step load: $Pa_{CO2} = 5$ mmHg) was imposed on a biological closed feedback loop, using the open-loop transfer functions determined in this study. In the simulation, when TG becomes excessively large, the ventilatory response to a change in Pa_{CO2} is accelerated, whereas an increase in gain alone leads to instability of the system causing an oscillatory phenomenon.
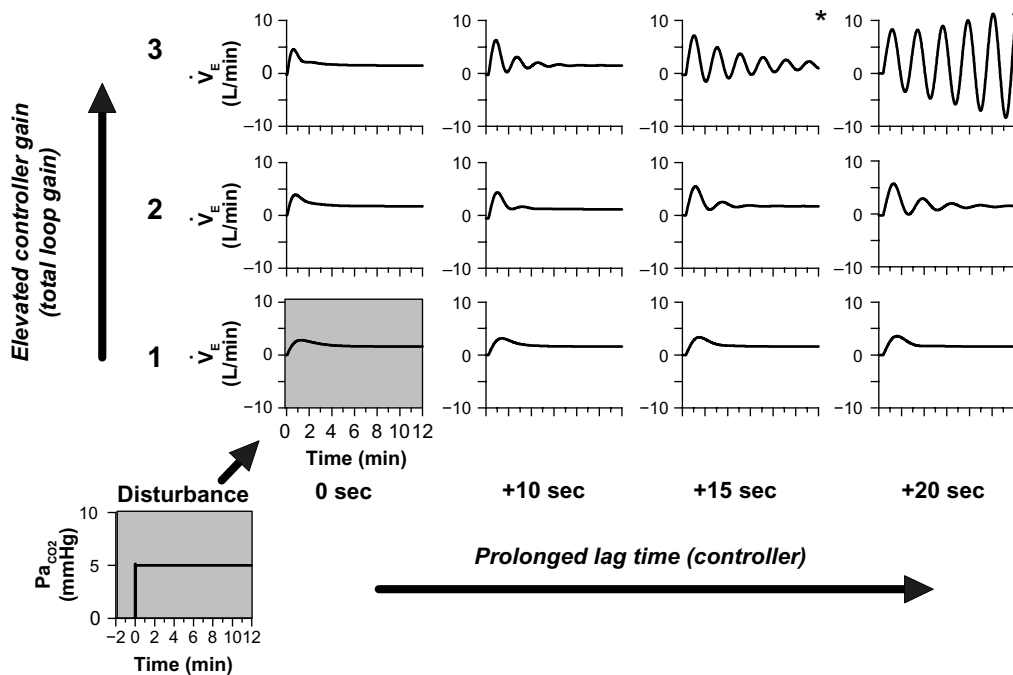

Figure 7. Simulations of changes in minute ventilation ($\dot{V}_E$) over time when a one-step perturbation (step load in arterial CO_2 partial pressure: $Pa_{CO2} = 5$ mmHg) was imposed on a biological closed feedback loop, using the open-loop transfer functions determined in this study. In the simulation, when the system gain (up to three-fold increase) and lag time (prolongation up to 20 seconds) are both increased within a physiologically relevant range, the condition for system oscillation is satisfied and periodic breathing occurs (*oscillation phenomenon).

The results of simulation based on the data obtained from healthy adults suggest that the respiratory chemoreflex system maintains blood gas homeostasis while fulfilling two polarizing requirements of rapidity and stability within the physiological range. When abnormality occurs in a part of the system, instability of the control system is amplified and may result in the manifestation of respiratory abnormalities such as Cheyne–Stokes respiration and periodic breathing.

In the future, quantitative analysis of the dynamic properties of the respiratory chemoreflex system may play a role in elucidating the adaptive mechanism of the exercise ventilatory response during training and the mechanism of respiratory abnormality in CHF. The open-loop transfer functions obtained can be used to simulate the closed-loop respiratory responses. For example, by changing various parameters within physiological ranges, it may be possible to reproduce abnormal respiration patterns associated with heart failure or with the phenomenon of hyperventilation during incremental loading exercise. In this manner, thought experimentation on the mechanism of respiratory responses under various pathophysiological conditions may be possible.

Study Limitations

First, the studied subjects were healthy, nonobese male. In contrast, patients with heart failure may have many risk factors, including obesity, and their characteristics may not be homogenous in the clinical setting. Therefore, the present data in the healthy volunteers, which had relatively homogenous characteristics, may not be directly applicable to the interpretation of the respiratory control in patients with heart failure. Notwithstanding the limitation, the fact that periodic breathing can be simulated by adjusting control parameters within physiological bounds will support the idea that respiratory abnormalities of CHF patients originate from an instability of respiratory feedback control system.

Second, the time-domain models for the step responses were determined empirically to mimic the measured step responses in the first and second experiments. While the models are useful to simulate the closed-loop dynamic response of the respiratory control, justifications of the models based on underlying physiological functions may become necessary to gain further insight into the pathogenesis of the respiratory abnormalities.

Conclusion

The system identification approach using a step-loading method allows determination of the dynamic and static properties of the controller and the plant of the respiratory chemoreflex feedback system. From the quantitative analysis and simulation of the dynamic function of the respiratory chemoreflex system, we attempted to explain the mechanism of periodic breathing in patients with CHF. This framework is potentially useful for understanding the mechanisms responsible for abnormal ventilation under various pathophysiological conditions.

REFERENCES

1. Kleber FX, Vietzke G, Wernecke KD, et al. Impairment of ventilatory efficiency in heart failure: prognostic impact. *Circulation*. 2000;101:2803–9.
2. Ponikowski P, Francis DP, Piepoli MF, et al. Enhanced ventilatory response to exercise in patients with chronic heart failure and preserved exercise tolerance: marker of abnormal cardiorespiratory reflex control and predictor of poor prognosis. *Circulation*. 2001;103:967–72.
3. Arzt M, Harth M, Luchner A, et al. Enhanced ventilatory response to exercise in patients with chronic heart failure and central sleep apnea. *Circulation*. 2003;107:1998–2003.
4. Cherniack NS, Longobardo GS. Cheyne-Stokes breathing. An instability in physiologic control. *N Engl J Med*. 1973;288:952–7.
5. Hanly P, Zuberi N, Gray R. Pathogenesis of Cheyne-Stokes respiration in patients with congestive heart failure: relationship to arterial PCO_2. *Chest*. 1993;104:1079–84.
6. Tkacova R, Hall ML, Liu PP, Fitzgerald FS, Bradley TD. Left ventricular volume in patients with heart failure and Cheyne-Stokes respiration during sleep. *Am J Respir Crit Care Med*. 1997;156:1549–55.
7. Andreas S, Hagenah G, Moller C, Werner GS, Kreuzer H. Cheyne-Stokes respiration and prognosis in congestive heart failure. *Am J Cardiol*. 1996;78:1260–4.
8. AlDabal L, BaHammam AS. Cheyne-Stokes respiration in patients with heart failure. *Lung*. 2010;188:5–14.
9. Francis DP, Willson K, Davies LC, Coats AJ, Piepoli M. Quantitative general theory for periodic breathing in chronic heart failure and its clinical implications. *Circulation*. 2000;31:2214–21.
10. Corrà U, Pistono M, Mezzani A, et al. Sleep and exertional periodic breathing in chronic heart failure: prognostic importance and interdependence. *Circulation*. 2006;113:44–50.
11. Dhakal BP, Murphy RM, Lewis GD. Exercise oscillatory ventilation in heart failure. *Trends Cardiovasc Med*. 2012;22:185–91. Review.
12. Solin P, Roebuck T, Johns DP, Walters EH, Naughton MT. Peripheral and central ventilatory responses in central sleep apnea with and without congestive heart failure. *Am J Respir Crit Care Med*. 2000;162:2194–200.
13. Wilcox I, McNamara SG. Abnormal breathing during sleep and increased central chemoreflex sensitivity in congestive heart failure. *Circulation*. 2000;12:102.
14. Milhorn HT Jr. *The Application of Control Theory to Physiological Systems*. Philadelphia: Saunders; 1966:147–66.
15. Berger AJ, Mitchell RA, Severinghaus JW. Regulation of respiration (third of three parts). *N Engl J Med*. 1977;297:194–201.
16. Cunningham DJC, Robbins PA, Wolff CB. Handbook of physiology. Macklem, PT, Mead J, editors. *Integration of Respiratory Responses to Changes in Alveolar Partial Pressures of CO_2 and O_2 and in Arterial pH*. Bethesda, MD: American Physiological Society; 1986:476–528.
17. Miyamoto T, Inagaki M, Takaki H, et al. Integrated characterization of the human chemoreflex system controlling ventilation, using an equilibrium diagram. *Eur J Appl Physiol*. 2004;93:340–6.
18. Ogoh S, Hayashi N, Inagaki M, Ainslie PN, Miyamoto T. Interaction between the ventilatory and cerebrovascular responses to hypo- and hypercapnia at rest and during exercise. *J Physiol*. 2008;586:4327–38.
19. Miyamoto T, Inagaki M, Takaki H, et al. Adaptation of the respiratory controller contributes to the attenuation of exercise hyperpnea in endurance-trained athletes. *Eur J Appl Physiol*. 2012;112:237–51.
20. Miyamoto T, Bailey DM, Nakahara H, Ueda S, Inagaki M, Ogoh S. Manipulation of central blood volume and implications for respiratory control function. *Am J Physiol Heart Circ Physiol*. 2014;306:H1669–78.

21. Sands SA, Edwards BA, Kee K, et al. Loop gain as a means to predict a positive airway pressure suppression of Cheyne-Stokes respiration in patients with heart failure. *Am J Respir Crit Care Med*. 2011;184:1067–75.

22. Lloyd BB, Cunningham DJC. Quantitative approach to the regulation of human respiration. Cunningham JC, Lloyd, BB editors. *The Regulation of Human Respiration*. Oxford, UK: Blackwell Scientific Publications; 1963:331–49.

23. Honda Y, Hayashi F, Yoshida A, Ohyabu Y, Nishibayashi Y, Kimura H. Overall "gain" of the respiratory control system in normoxic humans awake and asleep. *J Appl Physiol*. 1983;55:1530–5.

24. Cummin RC, Saunders KB. The ventilatory response to inhaled CO_2. Whipp BJ editor. *The Control of Breathing in Man*. Manchester: Manchester University Press; 1987:45–67.

25. Day TA, Wilson RJ. Brainstem P_{CO2} modulates phrenic responses to specific carotid body hypoxia in an in situ dual perfused rat preparation. *J Physiol*. 2007;578:843–57.

26. Mohan R, Duffin J. The effect of hypoxia on the ventilatory response to carbon dioxide in man. *Respir Physiol*. 1997;108:101–15.

27. Defares JG. Principles of feedback control and their application to the respiratory control system. Fenn WO, Rahn H, editors. *Handbook of Physiology, Respiration*. Vol 1. (Chap. Sect 3). Bethesda, MD: American Physiological Society; 1964:649–80.

28. Khoo MCK. Determinants of ventilatory in stability and variability. *Respir Physiol*. 2000;122:167–82.

29. Miyamoto T, Inagaki M, Takaki H, et al. Sensitized central controller of ventilation in rats with chronic heart failure contributes to hyperpnea little at rest but more during exercise. *Conf Proc IEEE Eng Med Biol Soc*. 2006;1:4627–30.

30. Xie A, Skatrud JB, Khayat R, Dempsey JA, Morgan B, Russell D. Cerebrovascular response to carbon dioxide in patients with congestive heart failure. *Am J Respir Crit Care Med*. 2005;172:371–8.

31. Robbins PA. Evidence for interaction between the contributions to ventilation from the central and peripheral chemoreceptors in man. *J Physiol*. 1988;401:503–18.